Model-free Adaptive Control for a Vapour-Compression Refrigeration Benchmark Process ⋆

Xian Yu, Zhongsheng Hou, and Xin Zhang

Advanced Control Systems Lab, School of Electronic and Information Engineering, Beijing Jiaotong University, Beijing 100044, China (e-mail: 15111013@bjtu.edu.cn; zhshhou@bjtu.edu.cn; 16120207@bjtu.edu.cn)

Abstract: A model-free adaptive control (MFAC) is applied to the Refrigeration Systems based on Vapour Compression of the BENCHMARK PID 2018. A SISO MFAC controller and a MIMO MFAC controller are designed to control the outlet temperature of evaporator secondary flux and the superheating degree of refrigerant at evaporator outlet by manipulating the expansion valve opening and the compressor speed. The two designed controllers are the pure data driven control methods without using any model information of the refrigeration process in the control implementation by virtue of the dynamic linearization technique, and the PID controllers can be considered as special cases of the two designed controllers. The qualitative and quantitative comparison results between the MFAC schemes and the default PID controllers given in the simulation platform provided by the Benchmark PID 2018 demonstrate the effectiveness of the two designed controllers.

Keywords: Model free adaptive control, dynamic linearization, vapour-compression refrigeration system, Benchmark PID 2018

1. INTRODUCTION

Refrigeration systems based on vapour compression are extensively used for air conditioning, refrigerating, heating and ventilating in buildings and household or industrial facilities [Rasmussen (2005); Bejarano et al. (2015a)]. The refrigeration systems hold a high percentage of worldwide energy consumption, therefore meaning a great impact on energy supply. And due to the decrease of fossil fuel reserves and non-renewable energy sources and the drastic increase of energy cost, their economy has become an urgent issue to concern. Hence an accurate and efficient control for refrigeration systems is the urgent requirement in terms of energy saving [Bejarano et al. (2017)].

A one-stage vapour-compression refrigeration process is a closed cycle with an evaporator, a condenser, a compressor, an expansion valve, connected with various pipes between them. The major control purposes are to guarantee that the cycle refrigeration capacity meets the thermal load at any moment and that the energy efficiency is as high as possible, despite disturbances, delay and partial load requirements. This objective can be achieved in practice by holding the outlet temperature of evaporator secondary flux $T_{e,sec,out}$ and the refrigerant superheating degree at evaporator outlet T_{SH} through manipulating the compressor speed N and the expansion valve opening A_v.

⋆ This work is supported by National Natural Science Foundation of China (NSFC) under Grants 61433002 and 61403025, and by Beijing Natural Science Foundation under Grant L161007 (Corresponding author: Zhongsheng Hou).

In recent years, many control methods have been proposed to the refrigeration systems in different applications. Most of the noteworthy control techniques are model predictive control [Franco et al. (2017); Hovgaard et al. (2012)], adaptive control [Rasmussen and Larsen (2011)], robust H_∞ control [Bejarano et al. (2015b)], decoupling control [Semsar-Kazerooni et al. (2008); Shen et al. (2010)], decentralized control [Jain et al. (2014); Shafiei et al. (2013)] and LQG control [Schurt et al. (2010)]. For almost all of the works mentioned above, the model information of refrigeration processes are demanded for control design, and the control design is mainly proceeded by modeling the refrigeration processes into linear models. It is generally known that the refrigeration systems exhibit strong nonlinear characteristics, highly coupled dynamics, inherent thermal inertia and dead times, which make the system modeling very difficult and time-consuming with the first principles or identification methods.

Facing the challenges brought by the modeling, the data-driven or model-free control methods for refrigeration processes have attracted increasing attention, and most of the data-driven control techniques applied successfully for the refrigeration systems in practice are PID control [Attaran et al. (2016); Bejarano et al. (2017)]. However, accurate models of refrigeration processes and effective controller designs are required for tuning PID controllers well. Furthermore, the tuning procedure can be time-consuming, expensive and difficult for the strong nonlinearity and high coupled dynamics of refrigeration processes. For other data-driven control applied in refrigeration processes, there exists few reports in current literatures. A data-driven predictive control [Shafiei et al. (2014)] was applied to refrigeration processes by using subspace identification under a direct load control scheme, but the linear structure information of model is required for this method.

Model-free adaptive control (MFAC) as one of typical data-driven control methods, initially proposed by Hou [Hou (1994)], and shaped in a systematic framework in [Hou and Jin (2013)], and with latest progresses and applications [Hou et al. (2017)], is applicable for a class of unknown discrete-time nonlinear systems by using the new concept, including the pseudo-partial-derivative or the pseudo-gradient vector for SISO nonlinear systems, and pseudo-Jaccobian matrix for MIMO nonlinear systems, and the dynamic linearization (DL) technique, including the compact form dynamic linearization (CFDL), the partial form dynamic linearization (PFDL) and the full form dynamic linearization(FFDL). By virtue of the DL technique, the corresponding works have been done in theory and practice from SISO to MIMO nonlinear systems [Hou and Jin (2013)].

The protype discrete-time SISO MFAC and the protype MIMO MFAC based on FFDL are applied in this paper for the vapour-compression refrigeration processes proposed in this Benchmark PID 2018. The designed SISO and MIMO FFDL-MFAC controllers only require the I/O data of controlled refrigeration processes. The detailed description on the process could found in the Benchmark PID 2018 [Bejarano et al. (2017)]. The two control inputs are A_v and N, and the two system outputs are $T_{e,sec,out}$ and T_{SH}. According to the MFAC theory, the controlled plants can be ensured to be closed-loop stable and convergent under some rational assumptions. Besides, the designed MIMO controller is able to handle the decoupling problem.

The rest of this paper is as follows. In section 2, a vapour-compression refrigeration process is briefly introduced and the DL between $T_{e,sec,out}$, T_{SH} and A_v, N is formulated. Section 3 presents the SISO and MIMO control design of refrigeration system. Some simulation results on a vapour-compression refrigeration benchmark process are shown in section 4. A conclusion is summarized in section 5.

2. PROBLEM FORMULATION

2.1 Principle of Refrigeration Processes

A typical one-stage vapour-compression refrigeration system is shown in Fig. 1, where the main components are the evaporator, condenser, variable speed compressor, expansion valve and various pipes connected between them. With the growth of electronics, variable speed compressors and electronic expansion valves have gradually replaced older single speed compressors and thermostatic expansion valves, respectively. These new components not only contribute to saving energy and reducing fluctuations in the manipulated variables, but also makes it possible to achieve a more accurate control [Bejarano et al. (2015b)].

The basic operating principle of a vapour-compression refrigeration system is as follows: 1) The refrigerant enters the evaporator at low temperature and pressure and absorbs heat from the secondary flux when evaporating it in the cold room; 2) Then the evaporated refrigerant is taken

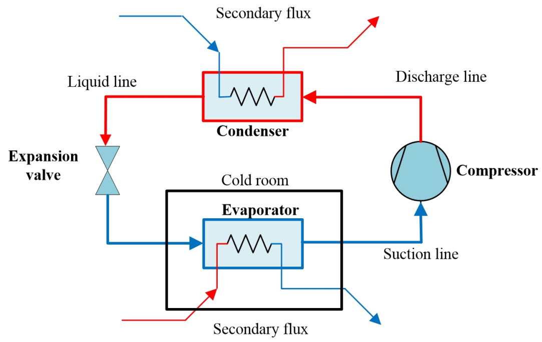

Fig. 1. Vapour-compression refrigeration system.

to the compressor where its pressure and temperature increase; 3) The temperature of the vapour firstly decreases after it enters to the condenser, and it may become subcooled liquid while removing heat to the condenser secondary flux; 4) Finally the refrigerant again enters into the evaporator at low pressure and temperature after it flows through the expansion valve.

In order to guarantee the cycle refrigeration capacity still achieves the thermal load at any moment, a practical way is to hold the $T_{e,sec,out}$ at its referred values, once given its inlet temperature. Since there exists two control inputs N and A_v to be manipulated, a secondary control purpose is to maintain as high as possible energy efficiency, which in this area is denoted by the Coefficient of Performance (COP) [Bejarano et al. (2017)]. In order to hold as high as possible COP value, a preferably low T_{SH} should be kept.

2.2 Dynamic Linearization for Refrigeration Processes

Referred to [Bejarano et al. (2015b)], it is known the model of vapour-compression refrigeration system is a high dimensional system with complex nonlinearity, which has restricted the implementation of model-based control methods. Modeling the refrigeration process is very difficult and time-consuming with first principles or identification methods for its high nonlinearity, and the corresponding controller structure designed by model-based control methods would definitely become much complex. In order to reduce computational burden for the controller design, the regular way for model-based control methods is to adopt model reduction or controller reduction. However, this way yields the problems of unmodeled dynamics and non-robust control. For robust controller design, it is demanded for the quantitative upper bound or qualitative expression of uncertainty of a controlled plant, which can not be provided by a theoretically modeling method.

The problem of unmodeled dynamics does not exist under the framework of MFAC by using the DL technique, since all useful information is included in the I/O data, and the DL process to the controlled plant does not omit any data or high order terms. Its details for vapour-compression refrigeration processes are presented as follows.

According to the Benchmark PID 2018 [Bejarano et al. (2017)], $T_{e,sec,out}$ is controlled by A_v and T_{SH} is controlled by N. Then the dynamic processes between $T_{e,sec,out}$ and A_v, T_{SH} and N can be expressed by the following discrete-time SISO nonlinear system in a general form

$$y_i(k{+}1){=}f_i\left(y_i(k),\cdots,y_i(k{-}n_{y_i}),u_i(k),\cdots,u_i(k{-}n_{u_i})\right), \quad (1)$$

where $i=1,2$; $y_1(k)$ and $y_2(k)$ are $T_{e,sec,out}(k)$ and $T_{SH}(k)$ at the time instant k, respectively; $u_1(k)$ and $u_2(k)$ are $A_v(k)$ and $N(k)$, respectively; the two positive integers n_{y_1} and n_{y_2} denote unknown orders of $y_1(k)$ and $y_2(k)$, respectively; the two positive integers n_{u_1} and n_{u_2} denote unknown orders of $u_1(k)$ and $u_2(k)$, respectively; $f_1(\cdot)$ and $f_2(\cdot)$ are unknown nonlinear functions.

Equation (1) is the SISO relationship between the system outputs and control inputs, and the effect of their coupling are not explicitly described. The MIMO description between $T_{e,sec,out}$, T_{SH} and A_v, N, considering with the complicated coupling effect explicitly, can be considered as the following discrete-time MIMO nonlinear system

$$\boldsymbol{y}(k+1)=\boldsymbol{f}\left(\boldsymbol{y}(k),\cdots,\boldsymbol{y}(k-n_y),\boldsymbol{u}(k),\cdots,\boldsymbol{u}(k-n_u)\right), \quad (2)$$

where $\boldsymbol{y}(k+1)=[y_1(k),y_2(k)]^T$; $\boldsymbol{u}(k)=[u_1(k),u_2(k)]^T$; n_y and n_u denote unknown orders of $\boldsymbol{y}(k)$ and $\boldsymbol{u}(k)$; $\boldsymbol{f}(\cdot)=[f_1(\cdot),f_2(\cdot)]^T$ is an unknown vector function.

Referred to literature [Hou and Jin (2011b)], (1) can be equivalently expressed by the following FFDL data model for the SISO nonlinear system

$$\Delta y_i(k+1)=\boldsymbol{\phi}_i^T(k)\Delta\boldsymbol{H}_i(k), \quad (3)$$

where $\Delta y_i(k+1)=y_i(k+1)-y_i(k)$; $\boldsymbol{\phi}_i(k)=[\phi_{i,1}(k),\cdots,\phi_{i,L_{i,y}+L_{i,u}}(k)]^T$ is unknown and bounded vector, called the pseudo gradient (PG); $\Delta\boldsymbol{H}_i(k)=[\Delta y_i(k),\cdots,\Delta y_i(k-L_{i,y}+1),\Delta u_i(k),\cdots,\Delta u_i(k-L_{i,u})+1]^T$, $\Delta u_i(k)=u_i(k)-u_i(k-1)$; $L_{i,y}$ and $L_{i,u}$ are pseudo orders of $f_i(\cdot)$, which implies the amount of information about system output and control input at previous time.

Analogy with (3), (2) can be equivalently transformed into the following FFDL data model [Hou and Jin (2011a)]

$$\Delta\boldsymbol{y}(k+1)=\boldsymbol{\Phi}(k)\Delta\bar{\boldsymbol{H}}(k), \quad (4)$$

where $\Delta\boldsymbol{y}(k+1)=\boldsymbol{y}(k+1)-\boldsymbol{y}(k)$; $\boldsymbol{\Phi}(k)=[\boldsymbol{\Phi}_1(k),\cdots,\boldsymbol{\Phi}_{L_y+L_u}(k)]$ is unknown and bounded matrix, called the pseudo partitioned Jacobian matrix (PPJM), $\boldsymbol{\Phi}_j(k)\in\mathbb{R}^{2\times2}$, $j=1,\cdots,L_y+L_u$; $\Delta\bar{\boldsymbol{H}}(k)=[\Delta\boldsymbol{y}^T(k),\cdots,\Delta\boldsymbol{y}^T(k-L_y+1),\Delta\boldsymbol{u}^T(k),\cdots,\Delta\boldsymbol{u}^T(k-L_u+1)]$, $\Delta\boldsymbol{u}(k)=\boldsymbol{u}(k)-\boldsymbol{u}(k-1)$, the two integers L_y and L_u are pseudo orders of $f(\cdot)$.

With (3) and (4), the corresponding SISO and MIMO FFDL-MFAC can be designed for the vapour-compression refrigeration system in next section.

3. CONTROLLER DESIGN

In this section, the SISO and MIMO FFDL-MFAC schemes based on (3) and (4) are designed to hold $T_{e,sec,out}$ and T_{SH} at their references $Ref\,T_{e,sec,out}$, and $Ref\,T_{SH}$, which are substituted by y_1^* and y_2^*, respectively for simplicity. The PFDL-MFAC scheme for SISO nonlinear system, and the CFDL-MFAC scheme for MIMO nonlinear system with rigorous analysis for the stability can be found in [Hou and Jin (2011b)] and [Hou and Jin (2011a)].

3.1 SISO Controller Design

For (1), consider the following control criterion function

$$J(u_i(k))=\left|y_i^*(k+1)-y_i(k+1)\right|^2+\lambda_i\left|\Delta u_i(k)\right|^2, \quad (5)$$

where $\lambda_i>0$ is a weight factor used as a penalty for $\Delta u_i(k)$.

Taking (3) into (5), letting $\partial J(u_i(k))/\partial u_i(k)$ be zero yields the following control law

$$\begin{aligned}u_i(k)=&u_i(k-1)+\frac{\rho_{L_{i,y}+1}\phi_{L_{i,y}+1}(k)\left(y_i^*(k+1)-y_i(k)\right)}{\lambda_i+\left|\phi_{L_{i,y}+1}(k)\right|^2}\\&-\frac{\phi_{L_{i,y}+1}(k)\sum_{m=1}^{L_{i,y}}\rho_{i,m}\phi_{i,m}(k)\Delta y_i(k-m+1)}{\lambda_i+\left|\phi_{L_{i,y}+1}(k)\right|^2}\\&-\frac{\phi_{L_{i,y}+1}(k)\sum_{m=L_{i,y}+2}^{L_{i,y}+L_{i,u}}\rho_{i,m}\phi_{i,m}(k)\Delta u_i(k+L_{i,y}-m+1)}{\lambda_i+\left|\phi_{L_{i,y}+1}(k)\right|^2},\end{aligned} \quad (6)$$

where $\rho_{j_i}\in(0,1]$ is a step size for generalizing the control law, $j_i=1,2,\cdots,L_{i,y}+L_{i,u}$.

Since PG $\boldsymbol{\phi}_i(k)$ is unknown, the next step is to estimate it. Firstly, an estimation criterion function is used as

$$\begin{aligned}J(\boldsymbol{\phi}_i(k))=&\left|y_i(k)-y_i(k-1)-\boldsymbol{\phi}_i^T(k)\Delta\boldsymbol{H}_i(k-1)\right|^2\\&+\mu_i\left\|\boldsymbol{\phi}_i(k)-\hat{\boldsymbol{\phi}}_i(k-1)\right\|^2,\end{aligned} \quad (7)$$

where $\mu_i>0$ is a weight factor used as a penalty for the change of PG. Then an estimation law about $\boldsymbol{\phi}_i(k)$ is obtained by applying a modified projection algorithm

$$\begin{aligned}\hat{\boldsymbol{\phi}}_i(k)=&\hat{\boldsymbol{\phi}}_i(k-1)\\&\frac{\eta_i\Delta\boldsymbol{H}_i(k-1)\left(y_i(k)-y_i(k-1)-\hat{\boldsymbol{\phi}}_i^T(k)\Delta\boldsymbol{H}_i(k-1)\right)}{\mu_i+\left\|\Delta\boldsymbol{H}_i(k-1)\right\|^2},\end{aligned} \quad (8)$$

where $\eta_i\in(0,2]$ is a step size for generalizing the estimation law (8), $\hat{\boldsymbol{\phi}}_i(k)$ is the estimation vector of $\boldsymbol{\phi}_i(k)$. In order to enhance the tracking ability of (8), a reset mechanism is applied, namely

$$\hat{\boldsymbol{\phi}}_i(k)=\hat{\boldsymbol{\phi}}_i(1), \quad (9)$$

if $\left\|\hat{\boldsymbol{\phi}}_i(k)\right\|\le\epsilon_i$, or $\left\|\Delta\boldsymbol{H}_i(k-1)\right\|\le\epsilon_i$, or sign $\left(\hat{\phi}_{L_{i,y}+1}(k)\right)\neq$ sign $\left(\hat{\phi}_{L_{i,y}+1}(1)\right)$, where $\epsilon_i>0$ is a small positive constant.

With (8) and (9), the control law (6) is rewritten as

$$\begin{aligned}u_i(k)=&u_i(k-1)+\frac{\rho_{L_{i,y}+1}\hat{\phi}_{L_{i,y}+1}(k)\left(y_i^*(k+1)-y_i(k)\right)}{\lambda_i+\left|\hat{\phi}_{L_{i,y}+1}(k)\right|^2}\\&-\frac{\hat{\phi}_{L_{i,y}+1}(k)\sum_{m=1}^{L_{i,y}}\rho_{i,m}\hat{\phi}_{i,m}(k)\Delta y_i(k-m+1)}{\lambda_i+\left|\hat{\phi}_{L_{i,y}+1}(k)\right|^2}\\&-\frac{\hat{\phi}_{L_{i,y}+1}(k)\sum_{m=L_{i,y}+2}^{L_{i,y}+L_{i,u}}\rho_{i,m}\hat{\phi}_{i,m}(k)\Delta u_i(k+L_{i,y}-m+1)}{\lambda_i+\left|\hat{\phi}_{L_{i,y}+1}(k)\right|^2},\end{aligned} \quad (10)$$

Remark 1: It is worthy of special attention that a PID controller is a special case of (10), since (10) can be transformed into the PID controller when letting $L_{i,y}=2$ and $L_{i,u}=0$ [Hou and Jin (2013)]. Furthermore, the parameters ρ_{j_i}, λ_i and the initial PG in (10) can be tuned by using some data-driven control methods, like PID, iterative feedback tuning (IFT) [Hjalmarsson et al. (1998)] and virtual reference feedback tuning (VRFT) [Campi et al. (2000)].

Remark 1 states that (10) can be transformed into the PID controller as shown in the following

$$\begin{aligned} u_i(k)=&u_i(k-1)+K_{i,P}\left(1+\frac{T_s}{K_{i,I}}+\frac{K_{i,D}}{T_s}\right)e_i(k) \\ &-K_{i,P}\left(1+2\frac{K_{i,D}}{T_s}\right)e_i(k-1)+K_{i,P}\frac{K_{i,D}}{T_s}e_i(k-2) \end{aligned} \tag{11}$$

where $K_{i,P}$, $K_{i,I}$, $K_{i,D}$ and T_s are the proportion, integration, differentiation and sampling time respectively. The next is the details. Transform (10) into

$$\begin{aligned} u_i(k)=&u_i(k-1)+\left(\frac{\rho_{i,3}\hat{\phi}_{i,3}(k)}{\lambda_i+\left|\hat{\phi}_{i,3}(k)\right|^2}+\frac{\rho_{i,1}\hat{\phi}_{i,3}(k)\hat{\phi}_{i,1}(k)}{\lambda_i+\left|\hat{\phi}_{i,3}(k)\right|^2}\right)e_i(k) \\ &+\left(\frac{\rho_{i,2}\hat{\phi}_{i,3}(k)\hat{\phi}_{i,2}(k)}{\lambda_i+\left|\hat{\phi}_{i,3}(k)\right|^2}-\frac{\rho_{i,1}\hat{\phi}_{i,3}(k)\hat{\phi}_{i,1}(k)}{\lambda_i+\left|\hat{\phi}_{i,3}(k)\right|^2}\right)e_i(k-1) \\ &-\frac{\rho_{i,2}\hat{\phi}_{i,3}(k)\hat{\phi}_{i,2}(k)}{\lambda_i+\left|\hat{\phi}_{i,3}(k)\right|^2}e_i(k-2), \end{aligned} \tag{12}$$

under the condition with $y_i^*(k+1)=\text{const}$ when letting $L_{i,y}=2$ and $L_{i,u}=0$, where $e_i(k)=y_i^*(k)-y_i(k)$. Comparing the right side of equation (11) and (12), it is obvious that (10) can be transformed into (11).

3.2 MIMO Controller Design

For the MIMO nonlinear system (2), the control criterion function is considered as

$$J(\boldsymbol{u}(k))=\left\|\boldsymbol{y}^*(k+1)-\boldsymbol{y}(k+1)\right\|^2+\lambda\left\|\Delta\boldsymbol{u}(k)\right\|^2, \tag{13}$$

where $\boldsymbol{y}^*(k+1)=[y_1^*(k+1), y_2^*(k+1)]^T$, $\lambda>0$ is a weight factor. Taking (4) into (13) and letting $\partial J(\boldsymbol{u}(k))/\partial\boldsymbol{u}(k)$ be zero gives the following control law

$$\begin{aligned} \boldsymbol{u}(k)=&\boldsymbol{u}(k-1)+\frac{\rho_{L_y+1}\boldsymbol{\Phi}_{L_y+1}^T(k)\left(\boldsymbol{y}^*(k+1)-\boldsymbol{y}(k)\right)}{\lambda_i+\left\|\boldsymbol{\Phi}_{L_y+1}(k)\right\|^2} \\ &-\frac{\boldsymbol{\Phi}_{L_y+1}^T(k)\sum_{m=1}^{L_y}\rho_m\boldsymbol{\Phi}_m(k)\Delta\boldsymbol{y}(k-m+1)}{\lambda_i+\left\|\boldsymbol{\Phi}_{L_y+1}(k)\right\|^2} \\ &-\frac{\boldsymbol{\Phi}_{L_y+1}^T(k)\sum_{m=L_y+2}^{L_y+L_u}\rho_m\boldsymbol{\Phi}_m(k)\Delta\boldsymbol{u}(k+L_y-m+1)}{\lambda_i+\left\|\boldsymbol{\Phi}_{L_y+1}(k)\right\|^2}, \end{aligned} \tag{14}$$

where $\rho_j\in(0,1]$ is a step size, $j=1,\cdots,L_y+L_u$.

Analogy with PG, an estimation criterion function over the PPJM $\boldsymbol{\Phi}(k)$ in (14) is considered as

$$\begin{aligned} J(\boldsymbol{\Phi}(k))=&\left\|\boldsymbol{y}(k)-\boldsymbol{y}(k-1)-\boldsymbol{\Phi}(k)\Delta\bar{\boldsymbol{H}}(k-1)\right\|^2 \\ &+\mu\left\|\boldsymbol{\Phi}(k)-\boldsymbol{\Phi}(k-1)\right\|^2, \end{aligned} \tag{15}$$

where $\mu>0$ is a weight factor. Then applying a modified projection algorithm for (15) yields

$$\begin{aligned} \hat{\boldsymbol{\Phi}}(k)=&\hat{\boldsymbol{\Phi}}(k-1) \\ &\frac{\eta\left(\boldsymbol{y}(k)-\boldsymbol{y}(k-1)-\hat{\boldsymbol{\Phi}}(k)\Delta\bar{\boldsymbol{H}}(k-1)\right)\Delta\bar{\boldsymbol{H}}^T(k-1)}{\mu+\left\|\Delta\bar{\boldsymbol{H}}(k-1)\right\|^2}, \end{aligned} \tag{16}$$

where $\eta\in(0,2]$ is a step size for generalizing the estimation law (16), $\hat{\boldsymbol{\Phi}}(k)$ is the estimation matrix of $\boldsymbol{\Phi}(k)$. In order to enhance the tracking ability of (16), two reset mechanisms are applied, namely

$$\hat{\phi}_{ii,L_y+1}(k)=\hat{\phi}_{ii,L_y+1}(1), \tag{17}$$

if $\left\|\hat{\phi}_{ii,L_y+1}(k)\right\|<b$, or $\left\|\hat{\phi}_{ii,L_y+1}(k)\right\|>\alpha b$, or $\operatorname{sign}\left(\hat{\phi}_{ii,L_y+1}(k)\right)\neq\operatorname{sign}\left(\hat{\phi}_{ii,L_y+1}(1)\right)$,

$$\hat{\phi}_{ii_1,L_y+1}(k)=\hat{\phi}_{ii_1,L_y+1}(1), \tag{18}$$

if $\left\|\hat{\phi}_{ii_1,L_y+1}(k)\right\|>b_1$, or $\operatorname{sign}\left(\hat{\phi}_{ii_1,L_y+1}(k)\right)\neq\operatorname{sign}\left(\hat{\phi}_{ii_1,L_y+1}(1)\right)$, where $\alpha>0$ is a small positive constant.

$$\begin{aligned} \boldsymbol{u}(k)=&\boldsymbol{u}(k-1)+\frac{\rho_{L_y+1}\hat{\boldsymbol{\Phi}}_{L_y+1}^T(k)\left(\boldsymbol{y}^*(k+1)-\boldsymbol{y}(k)\right)}{\lambda_i+\left\|\hat{\boldsymbol{\Phi}}_{L_y+1}(k)\right\|^2} \\ &-\frac{\hat{\boldsymbol{\Phi}}_{L_y+1}^T(k)\sum_{m=1}^{L_y}\rho_m\hat{\boldsymbol{\Phi}}_m(k)\Delta\boldsymbol{y}(k-m+1)}{\lambda_i+\left\|\hat{\boldsymbol{\Phi}}_{L_y+1}(k)\right\|^2} \\ &-\frac{\hat{\boldsymbol{\Phi}}_{L_y+1}^T(k)\sum_{m=L_y+2}^{L_y+L_u}\rho_m\hat{\boldsymbol{\Phi}}_m(k)\Delta\boldsymbol{u}(k+L_y-m+1)}{\lambda_i+\left\|\hat{\boldsymbol{\Phi}}_{L_y+1}(k)\right\|^2}, \end{aligned} \tag{19}$$

Remark 2: Analogy with the remark 1, a multivariable PID controller is a special case of (19), since (19) can be transformed into the multivariable PID controller when letting $L_y=2$ and $L_u=0$. And the parameters in (19) can be also tuned by using the multivariable PID, IFT and VRFT. What's more, the novel controller-dynamic-linearization-based MFAC [Hou and Zhu (2013)] can also be applied to the vapour-compression refrigeration systems.

4. SIMULATION RESULTS

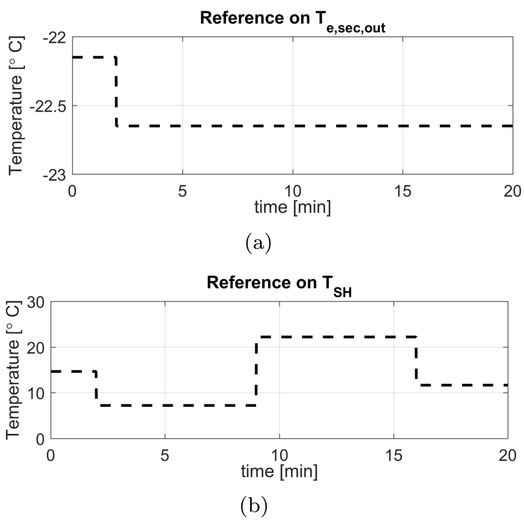

Fig. 2. References on controlled variables.

The qualitative and quantitative simulation results of the designed SISO FFDL-MFAC and MIMO FFDL-MFAC controllers are shown in this section, comparing them to the default PID controller and the multivariable PID controller provided in the Benchmark PID 2018, respectively. The sampling time is 1s and the terminate time

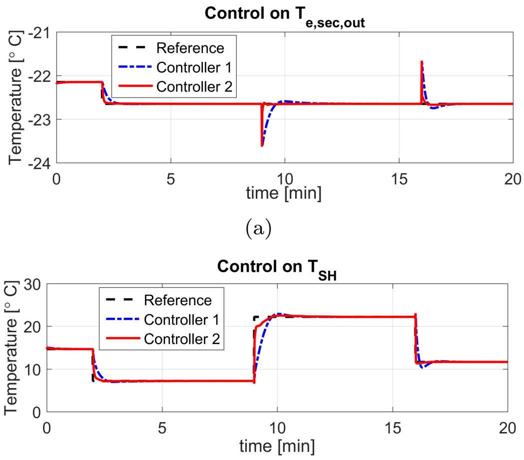

(b)

Fig. 3. Tracking performance for SISO control.

is $t_{end} = 1200s$ (20 minutes). The SISO FFDL-MFAC controller is designed to control $T_{e,sec,out}$ and T_{SH} by manipulating Av and N, respectively. And the MIMO FFDL-MFAC controller simultaneously manipulates Av and N for controlling $T_{e,sec,out}$ and T_{SH}. For the two applied controllers, the pseudo orders are $L_{i,y} = L_y = 2$ and $L_{i,u} = L_u = 1$. Thereafter, the proposed MFAC controller is called by controller 2, abbreviated as C_2 and the controller provided in the Benchmark is labelled by controller 1, abbreviated as C_1, both for SISO and MIMO, respectively. The desired outputs of the controlled vapour-compression refrigeration system are shown by Fig. 2. Please find the other settings for the vapour-compression refrigeration system provided by [Bejarano et al. (2017)].

Table 1. Indices for decentralized control

Index	Values
$\mathrm{RIAE_1(C_2, C_1)}$	0.2289
$\mathrm{RIAE_2(C_2, C_1)}$	0.3516
$\mathrm{RITAE_1(C_2, C_1}, t_{c1}, t_{s1})$	1.0495
$\mathrm{RITAE_2(C_2, C_1}, t_{c2}, t_{s2})$	0.3267
$\mathrm{RITAE_2(C_2, C_1}, t_{c3}, t_{s3})$	0.6223
$\mathrm{RITAE_2(C_2, C_1}, t_{c4}, t_{s4})$	0.1593
$\mathrm{RIAVU_1(C_2, C_1)}$	1.0029
$\mathrm{RIAVU_2(C_2, C_1)}$	0.9030
$\mathrm{J(C_2, C_1)}$	0.5393

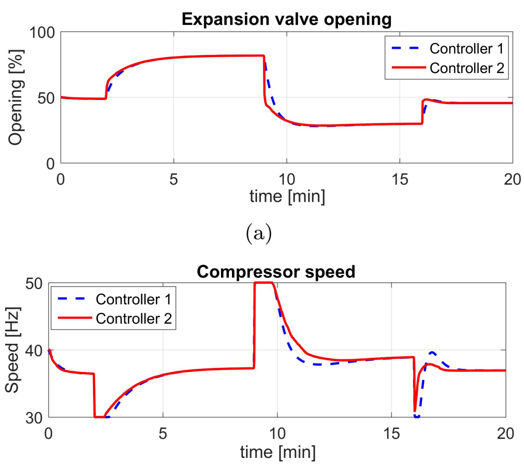

(b)

Fig. 4. Controlled inputs for SISO control.

Eight performance indices and one combined index are evaluated. The first two indices are the Ratios of Integrated Absolute Error (RIAE) for $T_{e,sec,out}$ and T_{SH}. The third is the Ratio of Integrated Time multiplied Absolute Error (RITAE) for $T_{e,sec,out}$ considering the sudden change in its reference, as shown in Fig. 2(a). The fourth, fifth and sixth indices are the RITAE for T_{SH} considering the three sudden changes in its reference, as shown in Fig. 2(b). The seventh and eighth indices are the Ratios of Integrated Absolute Variation of Control signal (RIAVU) for Av and N. The combined index is the mean value of the eight individual indices using a weighting factor for each index.

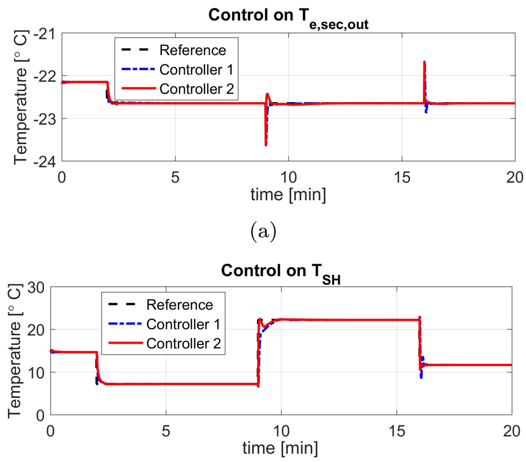

(b)

Fig. 5. Tracking performance for MIMO control.

The simulation results and the quantitative comparison indices for SISO control are presented in Fig.3, Fig. 4 and Table 1. As shown in Fig. 3 and Fig. 4, C_2 achieves better tracking performances both on $T_{e,sec,out}$ and T_{SH} and the corresponding control efforts for Av and N are lower than C_1, which are confirmed by Table 1. Only the third index is a little greater than 1. Furthermore, Table 1 shows that the overall performance of C_2 yields a better combined index $\mathrm{J(C_2, C_1)}$ than C_1. The simulation results and the quantitative comparison indices for MIMO control are presented in Fig.5, Fig. 6 and Table 2. Although the fifth index in Table 2 is greater than 1, the rest of the eight indices are lower than 1, which means that C_2 gives tighter control on $T_{e,sec,out}$ and T_{SH} and yields lower control efforts on Av and N than C_1. Besides, Table 2 shows that C_2 achieves better combined index than C_1.

Table 2. Indices for multivariable control

Index	Values
$\mathrm{RIAE_1(C_2, C_1)}$	0.9156
$\mathrm{RIAE_2(C_2, C_1)}$	0.5892
$\mathrm{RITAE_1(C_2, C_1}, t_{c1}, t_{s1})$	0.2450
$\mathrm{RITAE_2(C_2, C_1}, t_{c2}, t_{s2})$	0.9898
$\mathrm{RITAE_2(C_2, C_1}, t_{c3}, t_{s3})$	0.8162
$\mathrm{RITAE_2(C_2, C_1}, t_{c4}, t_{s4})$	0.5284
$\mathrm{RIAVU_1(C_2, C_1)}$	0.9471
$\mathrm{RIAVU_2(C_2, C_1)}$	0.6760
$\mathrm{J(C_2, C_1)}$	0.6651

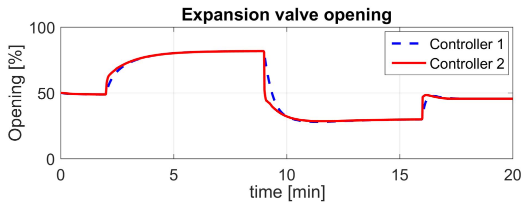

(a)

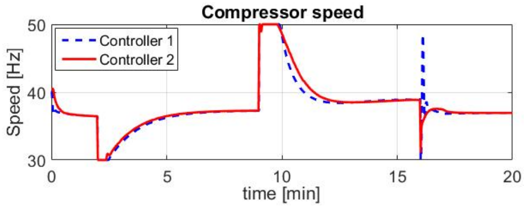

(b)

Fig. 6. Controlled inputs for MIMO control.

5. CONCLUSION

The SISO and MIMO FFDL-MFAC are applied in this paper for a vapour-compression refrigeration benchmark process. The main features for the proposed control methods are that the model information of the refrigeration system is not required and only the I/O data of the controlled plant is used for the controller design. And the MFAC controllers are simple, which makes them easy to be implemented with better performance, larger scope of applications [Hou, Chi and Gao, 2017], simpler parameter tuning, and similar computing speed to the traditional PID controllers.

REFERENCES

Attaran, S.M., Yusof, R., and Selamat, H. (2016). A novel optimization algorithm based on epsilon constraint-rbf neural network for tuning pid controller in decoupled hvac system. *Applied Thermal Engineering*, 99, 613–624.

Bejarano, G., Alfaya, J.A., Ortega, M.G., and Rubio, F.R. (2015a). Multivariable analysis and h_∞ control of a one-stage refrigeration cycle. *Applied Thermal Engineering*, 91, 1156–1167.

Bejarano, G., Alfaya, J.A., Ortega, M.G., and Rubio, F.R. (2015b). Multivariable analysis and h_∞ control of a one-stage refrigeration cycle. *Applied Thermal Engineering*, 91, 1156–1167.

Bejarano, G., Alfaya, J.A., Rogrĺguez, D., Ortega, M.G., and Morilla, F. (2017). Benchmark pid 2018. http://servidor.dia.uned.es/ fmorilla/benchmarkPID2018/.

Campi, M.C., Lecchini, A., and Savaresi, S.M. (2000). Virtual reference feedback tuning (vrft): a new direct approach to the design of feedback controllers. In *3t IEEE Conference on Decision and Control*, 623–629. Sydney, Australia.

Franco, I.C., Schmitz, J.E., Costa, T.V., Fileti, A.M.F., and Silva, F.V. (2017). Development of a predictive control based on takagi-sugeno model applied in a nonlinear system of industrial refrigeration. *Chemical Engineering Communications*, 204, 39–54.

Hjalmarsson, H., Gevers, M., and Gunnarsson, S. (1998). Iterative feedback tuning–theory and applications. *IEEE Control Systems*, 18, 26–41.

Hou, Z.S. (1994). *Parameter identification, adaptive control and model-free learning adaptive control for nonlinear systems.* Ph.D. thesis, Northeastern University, Shenyang, China.

Hou, Z.S., Chi, R.H., and Gao, H.J. (2017). An overview of dynamic-linearization-based data-driven control and applications. *IEEE Transactions on Industrial Electronics*, 60, 4076–4090.

Hou, Z.S. and Jin, S.T. (2011a). Data driven model-free adaptive control for a class of mimo nonlinear discrete time systems. *IEEE Transactions on Neural Networks*, 22, 2173–2188.

Hou, Z.S. and Jin, S.T. (2011b). A novel data-driven control approach for a class of discrete-time nonlinear systems. *IEEE Transactions on Control Systems Technology*, 19, 1549–1558.

Hou, Z.S. and Jin, S.T. (2013). *Model Free Adaptive Control: Theory and Applications.* CRC Press, New York, America.

Hou, Z.S. and Zhu, Y.M. (2013). Controller-dynamic-linearization-based model free adaptive control for discrete-time nonlinear systems. *IEEE Transactions on Industrial Informatics*, 9, 2301–2309.

Hovgaard, T.G., Larsen, L.F., Edlund, K., and Jorgensen, J.B. (2012). Model predictive control technologies for efficient and flexible power consumption in refrigeration systems. *Energy*, 44, 105–116.

Jain, N., Koeln, J.P., Sundaram, S., and Alleyne, A.G. (2014). Partially decentralized control of large-scale variable-refrigerant-flowsystems in buildings. *Journal of Process Control*, 24, 798–819.

Rasmussen, B.P. (2005). *Dynamic modeling and advanced control of air conditioning and refrigeration systems.* Ph.D. thesis, University of Illinois, Urbana-Champaign, USA.

Rasmussen, H. and Larsen, L.F.S. (2011). Non-linear and adaptive control of a refrigeration system. *Iet Control Theory and Applications*, 5, 364–378.

Schurt, L.C., Hermes, C.J.L., and Neto, A.T. (2010). Assessment of the controlling envelope of a model-based multivariable controller for vapor compression refrigeration systems. *Applied Thermal Engineering*, 30, 1538–1546.

Semsar-Kazerooni, E., Yazdanpanah, M.J., and Lucas, C. (2008). Nonlinear control and disturbance decoupling of hvac systems using feedback linearization and backstepping with load estimation. *IEEE Transactions on Control Systems Technology*, 16, 918–929.

Shafiei, S.E., Izadi-Zamanabadi, R., Rasmussen, H., and Stoustrup, J. (2013). A decentralized control method for direct smart grid control of refrigeration systems. In *52nd IEEE Conference on Decision and Control*, 6934–6939. Florence, Italy.

Shafiei, S.E., Knudsen, T., Wisniewski, R., and Andersen, P. (2014). Data-driven predictive direct load control of refrigeration systems. *Iet Control Theory and Applications*, 9, 1022–1033.

Shen, Y., Cai, W.J., and Li, S. (2010). Normalized decoupling control for high-dimensional mimo processes for application in room temperature control hvac systems. *Control Engineering Practice*, 18, 652–664.